Macromolecules
ARTICLE

Macromolecules **2010**, *43*, 501–510 **501**
DOI: 10.1021/ma902103q

Thermoresponsive Micelles of Phenanthrene-α-end-labeled Poly(*N*-decylacrylamide-*b*-*N*,*N*-diethylacrylamide) in Water

Gema Marcelo,[†] Telmo J. V. Prazeres,[†,‡] Marie-Therese Charreyre,[‡,c] José M. G. Martinho,*[,†] and José Paulo S. Farinha*[,†]

[†]*Centro de Química-Física Molecular and IN-Institute for Nanoscience and Nanotechnology Instituto Superior Técnico, Av. Rovisco Pais, 1049-001 Lisboa, Portugal, and* [‡]*Unité Mixte CNRS-bioMérieux, ENS, 46 Allée d'Italie, 69364 Lyon Cedex 07, France.* [c]*Current address: Laboratoire Joliot-Curie et Laboratoire Ingenierie des Materiaux Polymeres, ENS, IFR128, 46 Allee d'Italie, 69364 Lyon Cedex 07, France.*

Received September 22, 2009; Revised Manuscript Received October 30, 2009

ABSTRACT: Block copolymers of poly(*N*-decylacrylamide-*b*-*N*,*N*-diethylacrylamide) (PDcA-*b*-PDEA), with different PDEA block lengths and a constant PDcA block labeled with a phenanthrene fluorescent dye at the PDcA α-chain-end were prepared by RAFT polymerization. These copolymers form star-like micelles in water, (critical micelle concentration below 0.1 g/L, determined using coumarine 153) with a PDcA insoluble core surrounded by a PDEA corona showing thermoresponsive properties. The kinetics of Förster resonance energy transfer (FRET) between the chain-end phenanthrene groups and anthracene loaded into the hydrophobic core of the micelles in water, was analyzed using a new model for energy transfer in spherical nanodomains. This model takes into account the Poisson distribution of the acceptors in the micelle population and the existence of two phenanthrene states with different fluorescence lifetimes. The analysis yields the radius of the micelle core, $R_c = 2.7 \pm 0.1$ nm, with no need for deuteration of the core block. The result is compared with the value obtained by extrapolation of the light scattering data using the star micelle model, R_c(DLS) = 3.0 nm. The model for star-like micelles also yields a solvent-corona interaction parameter that changes with temperature due to the thermoresponsive nature of PDEA.

Introduction

Amphiphilic block copolymers consist of sequences of two types of monomers (A and B) linked at a common junction. If the block copolymer is dissolved in a solvent selective for polymer A, the polymer will spontaneously form micelles with a corona of solvent-swollen A chains surrounding a core of insoluble B chains. A broad variety of applications have been suggested for these micelles, ranging from small-molecule delivery vehicles[1] to surface modification agents.[2] Their current and potencial applications, as well as the intrinsic interest in self-assembling systems have fostered the study of block copolymer micelles.[3]

Much effort has been put into the design of systems with controlled response to an external trigger such as pH, light, temperature, or enzyme reaction.[4,5] Temperature is a commonly used stimulus for obtaining "intelligent" systems with potential biomedical and pharmaceutical applications. Polymers that respond to a temperature stimulus usually show a lower critical solution temperature (LCST) in water due to specific interactions with the solvent molecules. Above the LCST, the collapse of the chain from coil to globule is accompanied by a reduction of the polymer−solvent contacts, which are replaced by polymer−polymer interactions.[6] Amphiphilic diblock copolymers having one hydrophobic block and one thermoresponsive block form micelles below their volume phase transition temperature (T_{VPT}), which is close to the LCST of the thermoresponsive homopolymer. These micellar systems are stable below the T_{VPT} values, but become unstable above T_{VPT}, leading to multimicellar aggregates or clusters.[7] Another interesting system consists of chains with one hydrophilic block and one thermoresponsive block, forming micelles or vesicles above the T_{VPT}.[8]

*To whom correspondence should be addressed. E-mail: (J.M.G.M) jgmartinho@ist.utl.pt; (J.P.S.F.) farinha@ist.utl.pt.

Thermoresponsive polymers with LCST values close to physiological temperatures are specially attractive for applications in the biomedical and pharmaceutical fields.[9] An important class of such polymers are the poly(*N*-alkylacrylamides),[9−11] which exhibit a sharp and usually reversible transition from a hydrated to dehydrated form near their LCST in water.[12] Poly(*N*-isopropylacrylamide) (PNIPAM) is the most studied thermoresponsive water-soluble polymer,[13] however, PNIPAM is mildly nonbiocompatible while NIPAM monomer is strongly cytotoxic,[14] raising questions about their elimination from the body or the environment. To enhance biocompatibility, new thermoresponsive copolymers have been designed, with water-soluble main chains such as poly(2-ethyl-2-oxazoline), poly(2-isopropyl-2-oxazoline),[15] or poly(*N*,*N*′-diethylacrylamide) (PDEA).[16,17] PDEA has a LCST around 30−33 °C for the heteroactic form,[11,18] which depends on concentration,[19,20] tacticity,[19,21] molecular weight,[22] addition of salts,[20,23] addition of surfactants,[20] and incorporation of comonomers.[24] Microgels of PDEA have already been developed for drug delivery,[25] and solid-phase supports for peptide synthesis,[26] while block copolymers were developed as DNA condensation agents[27] and for DNA sequencing matrices.[28]

Reversible addition−fragmentation transfer (RAFT) polymerization is a versatile technique to prepare copolymers of controlled size and structure.[29] In the RAFT process most chains are initiated by thiocarbonylthio or related compounds (RAFT agents or chain transfer agents) which reversibly react with growing radicals via chain transfer reactions. To insert a dye at the α-terminus of a polymer chain in RAFT polymerization, the strategy adopted in this work is the use of a fluorescent RAFT agent.[30−34] Different fluorescent RAFT chain transfer agents were already used to prepare light-harvesting polymers.[30,31,35] These chain transfer agents were prepared either by ester formation

Published on Web 12/03/2009

Scheme 1. Combination of Light Scattering and Resonance Energy Transfer to Study the Aggregation Process of the PDcA-*b*-PDEA Block Copolymers Labeled with Phenanthrene at the α-Chain-End

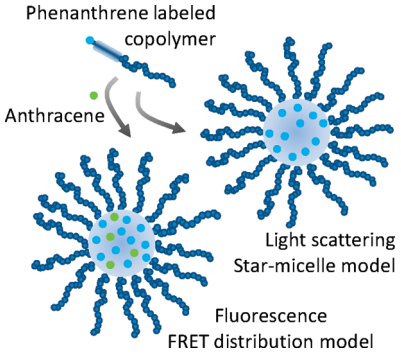

through carboxylic acid activation of a RAFT agent followed by reaction with an alcohol-derived fluorophore[30] or by using a 1:1 ratio of the RAFT agent and a fluorophore-labeled monomer.[31,32] More recently, a dithioester precursor was used to obtain biofunctionalized RAFT agents.[36] Here, we use this last strategy to prepare a phenanthrene-labeled RAFT agent (*N*-(4-(9-phenanthrenyl)butyl)-2-[[2-phenyl-1-thioxo]thio]-propanamide (PBTP)). Using PBTP we prepared a series of amphiphilic block copolymers of poly(*N*-decylacrylamide-*b*-*N*,*N*-diethylacrylamide), PDcA-*b*-PDEA, by RAFT polymerization using a sequential method.[29−31,37] First we prepared a PDcA block with a single phenanthrene dye at the α-chain-end using the PBTP RAFT agent. This block is then used as a macro chain transfer agent (macroCTA) to control the polymerization of the DEA monomer. In this way we were able to obtain a series of block copolymers with a hydrophobic PDcA block of the same length and hydrophilic PDEA blocks of different lengths. The hydrophobic block, PDcA, has brush-like alkyl chains, which are short enough to obtain micellar copolymer aggregates with a relatively fluid hydrophobic core. On the other hand, the hydrophilic PDEA chains forming the corona of the micelles show thermoresponsive properties in water.

Several techniques have been used to examine the structure of block copolymer micelles, from small angle scattering experiments involving light,[38,39] X-rays[40]and neutrons,[41] to transmission electron microscopy.[42] Here we report a combination of static and dynamic light scattering with resonance energy transfer to study the micelle formation process and structure of the dye-labeled PDcA-PDEA block copolymers (Scheme 1).

The molecular weight and the second virial coefficient of the micellar aggregates were obtained from static light scattering (SLS) data, and the hydrodynamic size was calculated by dynamic light scattering (DLS). The aggregation number of the block copolymer micelles obtained from the SLS results seems to be independent of the length of hydrophilic block, while the hydrodynamic dimensions of the micellar aggregates change with the length of the hydrophobic block and temperature. These results can be interpreted using a model for star-like micelles based on the packing of the blobs at the micelle shell.[39] While the aggregation number depends mainly on the core size (determined by the size of the hydrophobic block), the micelle shell thickness can be interpreted in terms of the extended conformation of the hydrophilic blocks anchored to the core.

On the other hand, to obtain information about the core structure of the PDcA-PDEA block copolymer micelles in water, we carried out resonance energy transfer experiments using the chain-end phenanthrene group as energy donor and anthracene as the acceptor. Anthracene is a hydrophobic dye and can be loaded into the hydrophobic core of the micelles. In this way, both the chain-end phenanthrene groups and the anthracene dye are confined to the core region. The rate of energy transfer from the donor to the acceptor is sensitive to the volume occupied by the dyes, and, with an appropriate model, can give information about the size of the micelle core, without the need for deuteration of the core block, necessary for neutron scattering experiments.

Förster resonance energy transfer (FRET) experiments have been used to obtain information on the core and core−corona interface of micelles composed by donor- and acceptor-labeled block copolymers.[43] Most experimental fluorescence decay curves obtained for these systems were analyzed using the Klafter and Blumen (KB) equation for energy transfer, initially derived for fractal systems[44] but applied phenomenologically to systems of restricted geometry.[45] To quantify the size of the micelle core we analyze the FRET results using a model derived from the general distribution models describing FRET in nanodomains,[46] applied to systems with inhomogeneous distributions of donor and acceptor dyes in domains with spherical geometry.[47−49] The model takes into account the size and shape of the domains in which the dyes are distributed and the variation in their concentration over the domains. In the analysis procedure, one must input a function describing the radial variation of the dye concentration and a cut off function describing the restricted domain where the dyes are confined. We consider that the number of chain-end phenanthrene groups in the core is constant and the number of loaded anthracene groups is given by a Poisson distribution with an average equal to the mean number of acceptors per micelle.

The paper is organized as follows: We begin with a brief description of the polymer synthesis and then present the analysis of the light scattering and the FRET experiments using the star−micelle model to describe the micelle corona and a distribution model to analyze the kinetics of FRET between dyes distributed in the micelle core.

Experimental Section

Materials. *N*,*N*-Diethylacrylamide (DEA) was purchased from Monomer−Polymer and Dajac Laboratories and distilled under reduced pressure in the presence of hydroquinone. *N*-Decylacrylamide (DcA) was synthesized as previously described.[50] The initiators 2,2′-azobis(2,4-dimethylvaleronitrile) (V-65) (WAKO, 98%) and 2,2′-azobis(isobutyronitrile) (AIBN) (Fluka, 98%) were purified by recrystallization from ethanol. The RAFT agent *N*-(4-(9-phenanthrenyl)butyl)-2-[[2-phenyl-1-thioxo]thio]propanamide (PBTP) was prepared from 4-(9-phenanthrenyl)butyl amine hydrochloride[51] using a procedure previously reported.[36,52] 1,4-Dioxane (Acros, 99%) was distilled over $LiAlH_4$ (110 °C), dimethyl sulfoxide (DMSO) (Aldrich, anhydrous, 99.9%), tetrahydrofuran (THF) (SDS, 99%), tetrabutylammonium bromide (TBAB) (Fluka, 99%), trioxane (Acros, 99%) Coumarin 153 (C153) (Fluka, 98%), Methanol (MeOH) (VWR), sodium dodecyl sulfate (SDS), Triton X-405, and cetyltrimethylammonium bromide (CTAB) were used as received.

Polymer Synthesis. PDcA-*b*-PDEA block copolymers with different PDEA block lengths and a PDcA block of the same length, labeled at the α-end with phenanthrene (Scheme 2) were synthesized using a sequential RAFT polymerization strategy, as previously described.[52,53] Shortly, the PDcA homopolymer (macroCTA) with an number average molecular weight of M_n = 2720 g/mol, corresponding to a polymerization degree of 11 and M_w/M_n = 1.13 (determined by MALDI−ToF MS) was prepared using PBTP as a chain transfer agent:[50] DcA (5.0 g, 23.8 mmol), PBTP (0.29 g, 0.64 mmol, chain transfer agent), AIBN (Fluka, 98%) previously purified by recrystallization from ethanol (10 mg, 0.063 mmol), 1,4-dioxane (Acros, 99%) previously distilled over $LiAlH_4$ at 110 °C (23.7 mL), and trioxane (Acros, 99%; 0.19 g, internal reference for ^{1}H NMR determination of monomer conversion) were introduced in a

Scheme 2. Chemical Structure of PDcA-*b*-PDEA Copolymers

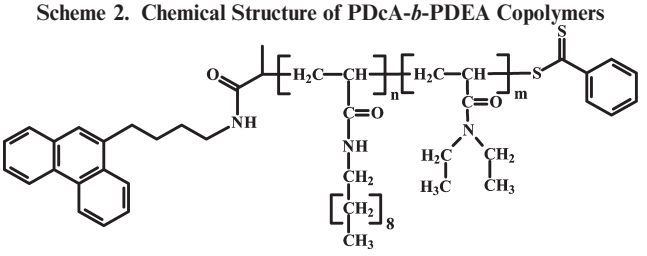

Table 1. Number and Weight Averaged Molecular Weight and Polydispersity Index (M_w/M_n) of Copolymers CP1 to CP5 Obtained by GPC−MALS

polymer	M_n/g mol^{-1}	M_w/g mol^{-1}	M_w/M_n
CP1	12700	12900	1.02
CP2	21200	22300	1.05
CP3	31600	32600	1.03
CP4	40300	39900	1.00
CP5	62300	63600	1.02

Schlenk tube equipped with a magnetic stirrer. We used [PBTP]/[AIBN] = 10 in order to get a low number of chains initiated by the initiator,[54] with an initial concentration of DcA of 1.0 M. The mixture was deoxygenated by four freeze−pump−thaw cycles and then under nitrogen, it was placed in a thermostated oil bath at 90 °C. The polymerization reaction was quenched at 1 h 30 min by cooling the shlenk in liquid nitrogen. Monomer conversion (21%) was determined by ^{1}H NMR. The homopolymer obtained was precipitated into a mixture of MeOH/H_2O (3:1 v/v) to remove the unreacted monomers, filtered, and dried under vacuum. The complete elimination of residual monomers was confirmed by ^{1}H NMR. The presence of the phenanthrene at the chain-end was confirmed by MALDI−ToF mass spectrometry, UV−vis spectroscopy, and fluorescence.[52]

This hydrophobic PDcA homopolymer was used as macroCTA for the RAFT polymerization of DEA in 1,4-dioxane ([DEA]$_0$ = 3.8 mol L^{-1}) at 70 °C under N_2 atmosphere, using V-65 initiator. The [macroCTA]/[V-65] ratios were kept equal to 9 in order to keep a low number of chains initiated by V-65. The concentration of macroCTA and/or the reaction time was varied in order to obtain copolymers with different PDEA block lengths. (Table 1) The final PDcA-*b*-PDEA copolymers were precipitated in cold petroleum ether (3 times) in order to remove unreacted monomer and macroCTA. The five final copolymers were recovered and dried under vacuum. The complete elimination of residual monomers was confirmed by ^{1}H NMR.

The molecular weight distributions of the hydrophobic polymer (Phe-PDcA macroCTA) and the copolymers were obtained by size exclusion chromatography (GPC) using a Waters 1515 isocratic HPLC pump with flow rate 1 mL min^{-1}, Waters 2410 refractive index detector, and a Styragel HR4E column. The relative molecular weights of the Phe-PDcA macroCTA were obtained in THF using polystyrene standards. The absolute molecular weight of the copolymers were obtained in DMF, using both a differential refractive index and a multiangle light scattering (miniDAWN TREOS from Wyatt) detectors. The differential refractive index of the copolymer was set equal to the value of PDEA in DMF, dn/dc = 0.081 mL g^{-1}.

The labeling efficiency for phenanthrene is expected to be higher than 90% since the [CTA]/[initiator] ratio was 10 in the synthesis of the macroCTA and 9 for the copolymerizations.

Thiol-Terminated Copolymers. The thiocarbonylthio group is known to be a fluorescence quencher of coumarin dyes,[50] and therefore, the copolymers used to determine the critical micelle concentration (cmc) were treated by a large excess of hexylamine (~100 equiv) in dichloromethane at room temperature during ca. 4 h.[55] The treated copolymers were precipitated several times in hexane in order to remove the excess of hexylamine and the secondary product from the aminolysis reaction. The orange or rose copolymers gave origin to white polymers with the thiol function at the ω-terminus. In control experiments, we verified the absence of the thiocarbonylthio absorption in the visible wavelenghts. Only the characteristic absorption of the phenanthrene derivative linked to the α-terminus of the copolymers was observed. The characteristic fluorescence lifetime of phenanthrene derivative in THF (ca. 47 ns) was obtained by time-resolved fluorescence, indicating the elimination of fluorescence quenching. This result is also supported by a previous observation in which the thiol group (SH) does not quench the fluorescence of C343.[50]

Micelle Preparation. The copolymer aqueous solutions used in the fluorescence and the DLS experiments were prepared using a solvent-assisted solubilization method in order to obtain monodisperse micelles, preventing the formation of large aggregates, and allowing us to uniformly solubilize C153 (cmc determination experiments) and anthracene (FRET experiments). Small volumes of cold water were added dropwise to concentrated solutions (~75 g/L) of copolymers CP1−CP5 dissolved in THF (a good solvent for both blocks), in small vails or light scattering tubes (immersed in an ice bath at ~2 °C), up to the required final volume. The final solutions contained always less than 2% v/v of THF.[56] Control experiments indicated that the low THF content does not interfere significantly in the properties of the micellar aggregates. The final aqueous solutions were always equilibrated at 4 °C for at least 24 h and stored at the same temperature. To prepare micelles containing the coumarine C153 dye or anthracene, the block copolymer and the dye were previous mixed in THF solution, before adding cold water.

Instrumentation. Static and dynamic light scattering measurements were performed in a Brookhaven instrument (BI-200SM Goniometer and BI-9000AT correlator) using a He−Ne laser (632.8 nm, 35 mW, model 127, Spectra Physics) and an avalanche photodiode detector. The measurements were carried out in glass cylindrical cells in order to simplify the corrections needed for refractive index variations, inside a vat containing decaline to minimize light refraction.

The normalized intensity autocorrelation function, $g^{(2)}(t)$, measured by DLS is related to the normalized time-correlation function of the electric field, $g^{(1)}(t)$, by the Siegert relation[57]

$$g^{(2)}(t) - 1 = \beta |g^{(1)}(t)|^2 \quad (1)$$

where t is the delay time and β (≤ 1) is a coherence factor which accounts for deviation from ideal correlation and is normally determined in the fitting procedure. For polydisperse scattering particles, the electric field correlation function is described by[58]

$$g^{(1)}(t) = \int_0^\infty \tau \Delta(\tau) \exp(-t/\tau)\, \mathrm{d}[\ln \tau] \quad (2)$$

where τ is the relaxation time and $\Delta(\tau)$ is the relaxation time distribution. The DLS data were analyzed using the analysis package CONTIN (Brookhaven) and a cumulant expansion[59] to determine the translational diffusion coefficient, from which the hydrodynamic radius (R_H) of the copolymer micelles is calculated using the Stokes−Einstein relationship for noninteracting spheres

$$R_H = \frac{kT}{6\pi\eta_0 D_0} \quad (3)$$

where k is the Boltzmann constant, T is the absolute temperature, η_0 is the solvent viscosity and D_0 is the diffusion coefficient at infinite dilution.

Steady-state fluorescence measurements were carried out with a SPEX Fluorolog F112A fluorimeter. The absorption UV−vis spectroscopy measurements were carried out in a Shimadzu

UV-3101PC UV−vis−NIR. The steady-state fluorescence spectra of C153 were acquired in a SLM-AMINCO 8100 Series 2 spectrofluorimeter. All spectra were corrected for background fluctuations.

Fluorescence decay measurements with picosecond resolution were obtained by the single photon timing technique in a setup previously described.[60] The experimental fluorescence decay curves were analyzed using software that simulates parametrized model decay curves and uses a nonlinear least-squares reconvolution method based on the Marquard algorithm[75] to compare the simulated curves with the experimental decays. For fluorescence and absorption measurements, the micelle solutions were deoxygenated by argon flow and kept at 4 °C.

Results and Discussion

The PDcA-PDEA block copolymers CP1−CP5 form star-like micelles in water, with a PDcA insoluble core surrounded by a PDEA corona. The micelles are spherical as expected from the small volume ratio of the compact PDcA block (M_n = 2720 g/mol) and the solvent swollen PDEA block (M_n = 12 720 g/mol to M_n = 62 310 g/mol). The micelles are prepared from block copolymers labeled with a phenanthrene fluorescent dye at the PDcA α-chain-end, so that the dyes become confined to the micelle hydrophobic core.

Critical Micelle Concentration. In order to determine the critical micelle concentration for the PDcA-*b*-PDEA block copolymers in water, we used coumarin 153 (C153), instead of the more commonly used pyrene dye. C153 has a number of advantages over pyrene for the determination of the cmc of block copolymer micelles in water. Indeed, the solubility of pyrene in water is very low (~10^{-7} M) and pyrene forms ground-state aggregates even at low concentrations in polar media. The fluorescence spectra is disturbed by the presence of fluorescent aggregates directly excited by the excitation light or formed in the excited state. This complicates the determination of the cmc based on the vibronic band structure, the pyrene monomer intensities or lifetimes, and the excimer to monomer fluorescence intensity ratio. On the other hand, C153 shows very clear variations in the fluorescence intensity and the wavelength of the fluorescence band maximum when going from apolar to polar environments. The solvatochromism of C153 has been studied by steady-state fluorescence and the solvent shifts are those expected for an electronic transition involving a large variation in the transition dipole moment.[61−63] C153 is a nearly ideal solvation probe with the S0 → S1 transition uncomplicated by other close states or interfering reactions (absence of overlapping between different excited states).[64] Therefore, in solvation studies, we can assume that the spectral shifts observed reflect only the energetics of solute−solvent interactions, without interference from other factors. In Figure 1 (top), we show the fluorescence intensity (fluorescence spectra) and the solvatochromic blue shift of C153 as the concentration of CP3 increases. Similar behavior has been observed for solutions of the other copolymers in water (CP1, CP2, CP4, CP5). The wavelengths at maximum fluorescence intensity and the fluorescence intensity are plotted as a function of the concentration of CP3 in Figure 1 (middle, bottom). At the critical micelle concentration (cmc) there is a pronounced decrease in wavelength values at the emission maximum and an increase in fluorescence intensity due to the increasing amount of C153 in the hydrophobic cores of micellar aggregates. The same method was used to determine the cmc values of the other copolymers giving values on the order of 0.02−0.07 g/L (maximum of intensity) and 0.03−0.08 g/L (wavelength of maximum intensity).

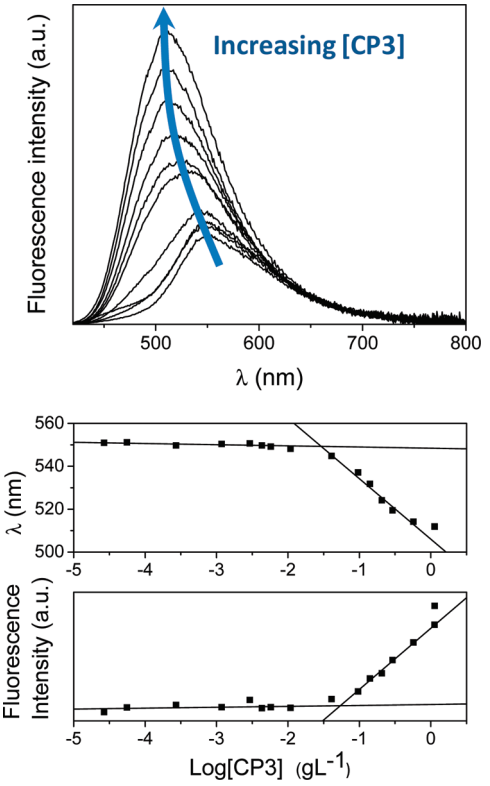

Figure 1. Fluorescence spectra of C153 in aqueous CP3 solutions (λ_{exc} = 410 nm; T = 20 °C; [C153] = 0.45 μM) (top). Plots of the wavelength at the maximum of the fluorescence band (middle) and the fluorescence intensity (bottom) of C153 as a function of CP3 concentration (g/L).

Micelle Aggregation Number and Second Virial Coefficient. A Zimm plot[65] of the static light scattering (SLS) data for the different block copolymers in water at 20 °C and concentrations above the cmc yields the values of the weight average micelle molecular weight (M_w) and second virial coefficient (A_2). SLS measurements for the PDcA-PDEA block copolymers in water were performed in the range of concentrations from ≈10 mg/mL up to the limit where multiple scattering was observed (40 mg/mL) and scattering angles from 90° to 140° in 10° increments. From the molecular weight determined for the micelles in water and the molecular weight of a single chain (Table 1) we calculate the weight average aggregation number (N_w^{agg}) of the micelles of CP2−CP5 (Table 2). The weight-averaged aggregation number is essentially independent of the molecular weight of the corona forming block, indicating that the packing of the bulky pDAc block in the core controls the aggregation number of the micelles, with no constrains imposed by the water-swollen corona chains. In fact, the micelle structure is essentially determined by the curvature arising from the relative sizes of the core and shell domains (which depends on the balance between the hydrophobic and hydrophilic interactions determining the surface area of the interface between the two domains), and the length and volume of the core block. For the polymers presented here, these factors remain constant as the corona block size changes.

The angular dependence of the scattered light is rather weak and it was not possible to calculate the micelle radius of gyration with accuracy. For particles smaller than $\lambda/20$, only a negligible phase difference exists between light emitted from the various scattering centers within a given particle, and the detected scattered intensity is almost independent of the scattering angle and only depends on the mass of the

Table 2. Molecular Weight, Second Virial Coefficient, and Aggregation Number of the Block Copolymer Micelles in Water at 20 °C

copolymer	micelle M_w (g/mol)	A_2 (cm^3 mol g^{-2})	R_{A_2} (nm)	aggregation number N_w^{agg}
CP2	8.15×10^5	8.6×10^{-4}	3.8	31
CP3	1.035×10^6	9.80×10^{-4}	4.7	30
CP4	1.766×10^6	1.12×10^{-3}	7.0	30
CP5	2.080×10^6	1.73×10^{-3}	9.0	27

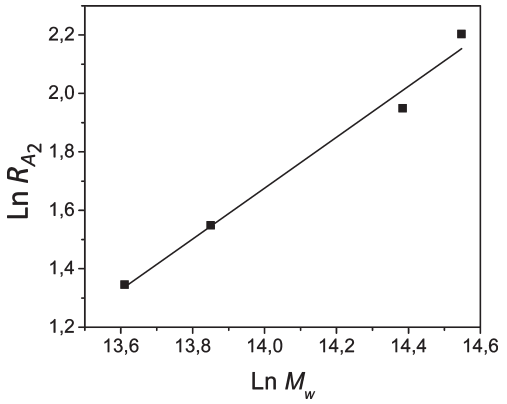

Figure 2. Hard-sphere virial radius, R_{A_2}, calculated from the second virial coefficient (A_2) and the molecular weight (M_w) of the micelles in water for copolymers with different PDEA hydrophilic block lengths (CP2−CP5) at 20 °C.

particle which is proportional to the total number of scattering centers in a particle.

The second virial coefficient, A_2, obtained for micelles of CP2−CP5 are small but positive and increase with the molecular weight of the hydrophilic block (Table 2) indicating that the intermicellar interaction is repulsive (the micelles are stable in solution) and that the micelles of copolymers with a larger hydrophilic length are more thermodynamically stable.

The second virial coefficient (A_2) can also be expressed as a hard-sphere virial radius, R_{A2}, calculated from A_2 and the molecular weight (M_w) of the micelles (N_A is the Avogadro number).[66]

$$R_{A_2} = \left(\frac{3M_w^2 A_2}{16\pi N_A}\right)^{1/3} \quad (4)$$

The R_{A_2} radius corresponds to a sphere where only the excluded volume effect has been taken into account. While for noninteracting spherical particles, the R_{A_2} values should be very close to the hydrodynamic radius R_H, the values of R_{A_2} calculated for the micelles of CP2−CP5 (Table 2 and Figure 2) are much smaller than the corresponding R_H values obtained by DLS (Table 3). This is expected for star-like block copolymer micelles, where the corona chains create a "soft" outer shell that provides steric stabilization of the micelles.

Variation of the Micelle Hydrodynamic Radius with Temperature. To evaluate the size polydispersity of the block copolymer micelles we calculated the ratio μ_2/Γ^2 of the second cumulant μ_2 to the square of the first cumulant Γ.[67] We find that μ_2/Γ^2 is on the order of 0.048−0.133 for the micelle samples investigated and using the approximations $\mu_2/\Gamma^2 \approx 0.25$ ($M_w/M_n - 1$) for Gaussian coils and $\mu_2/\Gamma^2 \approx 0.33$ ($M_w/M_n - 1$) for hard spheres we obtain $M_w/M_n = 1.2-1.5$ and $M_w/M_n = 1.1-1.4$, respectively.[58] These values indicate that the micelles obtained by self-assembling of the amphiphilic copolymers CP1−CP5 in water are monodisperse in size.

Table 3. Hydrodynamic Radii R_H of the Micelles in Water for Copolymers with Different PDEA Hydrophilic Block Lengths at Temperatures below the Volume Phase Transition of PDEA

	R_H (nm)				
T/°C	CP1	CP2	CP3	CP4	CP5
7	11.6	13.7	18.5	21.8	28.1
13	10.7	13.4	17.4	20.1	26.7
20		13.2	16.3	18.2	24.6
23			15.9		24.3
25			15.5		22.7

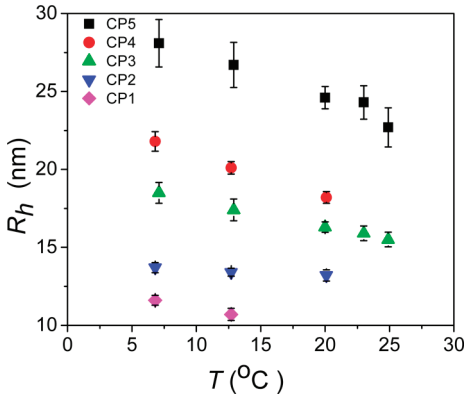

Figure 3. Hydrodynamic radii R_H of the micelles of PDcA-*b*-PDEA copolymers in water with different PDEA hydrophilic block lengths (CP1−CP5) determined by DLS at temperatures below the volume phase transition of PDEA, at a polymer concentration of 1.4 g/L.

The hydrodynamic radii R_H obtained by DLS of the micelles in water were measured at different temperatures for copolymers with different hydrophilic block length (Table 3). The diffusion coefficients exhibited no concentration dependence, and were taken as the average of several measurements at a copolymer concentration of 1.4 g/L (adjusted in order to have the most diluted concentration without significant interference of dust). Figure 3 shows plots of R_H of the micellar aggregates formed by copolymers CP1−CP5 at five temperatures (7, 13, 20, 23, and 25 °C).

R_H values are larger for micelles with larger corona block lengths. Also, R_H decreases for each polymer as the temperature increases and approaches the volume phase transition temperature T_{VPT} of PDEA. This change is more pronounced for micellar aggregates formed by copolymers with longer hydrophilic blocks. Measurements above this value revealed the formation of large micelle aggregates. The aggregation is almost reversible but some large aggregates remain after decreasing the temperature below T_{VPT}, with two populations being observed in the diameter distribution. Although the amount of aggregates remaining after lowering the temperature is probably small, the weighting of the particle distribution by the scattered light intensity (that depends on the square of the particle volume), increases their contribution to the diameter distribution and reduces the precision in the measurement of the micelle diameter. We also measured the size of the individual CP3 copolymers in water below the cmc for which we obtained an hydrodynamic radius $R_H = 6$ nm at 20 °C. This value corresponds to the chains in a coil conformation, more compact than the stretched conformation adopted by the polymer in the micelles.

Determination of the Micelle Core Radius: Star Micelle Model. The chains in the corona are in a semidilute condition, and the high surface density promotes chain stretching

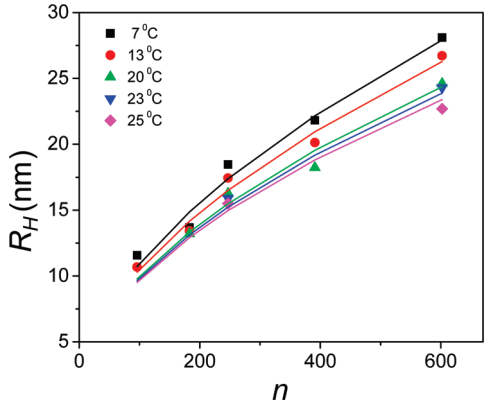

Figure 4. Hydrodynamic radii R_H of the micelles in water for copolymers with different PDEA hydrophilic block length n at temperatures below the volume phase transition of PDEA: 7, 13, 20, 23, and 25 °C.

(at 20 °C the hydrodynamic radius R_H = 6 nm of the CP3 copolymer below the cmc is smaller than the radius of the micelle shown in Table 3). The degree of extension of the chains is related to the quality of the solvent and the interface area *per* corona chain, s,[68] which can be calculated from the core radius and the number average aggregation number (N_n^{agg}) of the micelles $s = 4\pi R_{core}^2/N_n^{agg}$. If this area corresponds to a radius smaller than the radius of gyration of the free chains in the same solvent, $s^{1/2} < R_g$, the coils overlap at the surface and lead to stretching of the corona chains. The corona thickness L of star-like micelles, can be described by the discrete blob (DB) model[39] as a function of the scaling exponent ν (ν = 0.5 in conditions), the core radius and the corona chain length, expressed in terms of the number of monomers *per* statistical segment (N), the statistical segment length (a), and the micelle aggregation number

$$L_c^{DB} = \left[Na^{1/\nu} \frac{(1+2\Xi)^{1/\nu} - 1}{(2\Xi)^{1/\nu}} + R_{core}{}^{1/\nu} \right]^{\nu} - R_{core} \qquad (5)$$

where Ξ is defined as the ratio between the diameter of the first polymer chain blob in the corona and the radius of the micelle core

$$\Xi = \frac{2\sin(\gamma/2)}{1-\sin(\gamma/2)}$$
$$\cos\gamma = \left(\frac{\cos\alpha}{1-\cos\alpha}\right) \qquad (6)$$
$$\alpha = \pi\frac{N_n^{agg}+2}{3N_n^{agg}}$$

In Figure 4 we plot the hydrodynamic radii R_H of the micelles for copolymers with different PDEA hydrophilic blocks (of length n) in water, at different temperatures below their volume phase transition temperature. The micelle radius increases with the number of monomer units in the corona block and decreases as the temperature increases approaching the T_{VPT}. This behavior is well described by eqs 5,6, according to which L increases with N but decreases as the solvent quality for the chain decreases (lower values of the scaling exponent ν).

For the weight average aggregation number determined by SLS, N_w^{agg} = 30, we perform a global fit of all the results using eqs 5,6 (Figure 4). The fitting parameters are the core radius R_{core}, common to all polymers, the scaling exponent

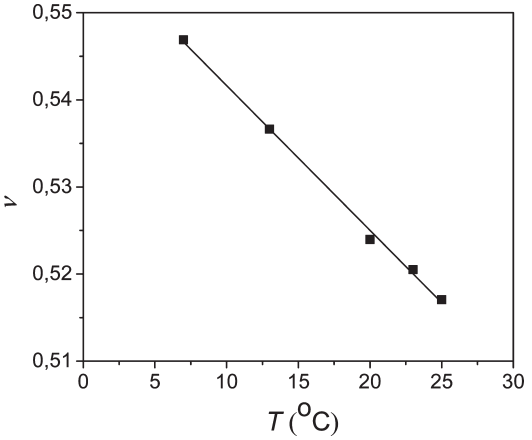

Figure 5. Scaling exponent ν obtained by fitting the hydrodynamic radii R_H of the micelles of copolymers with different PDEA hydrophilic block length n in water (Figure 3) to the DB model (eqs 5 and 6) for temperatures 7, 13, 20, 23, and 25 °C.

ν for each temperature and the statistical segment length of PDEA, b'. The obtained scaling exponent ν is plotted in Figure 5, the recovered core radius was R_{core} = 3.0 nm and the statistical PDEA segment length is b' = 0.60 nm. The later value is not published but is within the range expected for a flexible polymer. The scaling exponent ν is found to change almost linearly with temperature, assuming values slightly higher than for a flexible chain in θ conditions. This variation of ν with temperature is related to the change in solvent quality with temperature below the LCST of PDEA. In fact, extrapolating this trend to ν = 0.5 (θ condition), we obtain T = 35 °C, a value which is only slightly above the volume phase transition temperature of the PDEA shell, $T_{VTP} \approx$ 33 °C. For the aggregation number N_w^{agg} = 30, the PDcA block molar mass M_n = 2720 g/mol, and the core radius R_{core} = 3.0 nm, we obtained an estimated core density of d_{core} = 1.2 g/mL, similar to the values known for other flexible polymers.

Energy Transfer Kinetics in the Micelle Core. Förster[69] showed that, for a dipole−dipole coupling mechanism, the rate of energy transfer $w(r)$ between a donor and an acceptor depends on their separation distance r

$$w(r) = \frac{3\kappa^2}{2\tau_D}\left(\frac{R_0}{r}\right)^6 \qquad (7)$$

where τ_D is donor fluorescence lifetime in micelles labeled with donor only. R_0 is the critical Förster distance, with R_0 = 2.3 ± 0.1 nm for the present system,[47] and κ^2 is a dimensionless parameter related to the relative orientation of the donor and acceptor transition dipole moments. Since the donor is fixed at the end of the bulky PDcA chains, we assume that the dipoles are randomly oriented and fixed during the transfer time. In this case we can use the value κ^2 = 0.476.[70]

According to the distribution model for energy transfer in spherical systems,[47−49] the donor decay function for a delta-pulse excitation will be given by

$$I_D(t) = \exp\left(-\frac{t}{\tau_D}\right)\int_{V_s} C_D(r_D)\varphi(t,r_D) r_D^2\, \mathrm{d}r_D \qquad (8)$$

$$\varphi(t,r_D) = \exp\left(-\frac{2\pi}{r_D}\int_{R_e}^{\infty}\{1-\exp[-w(r)t]\}\left[\int_{|r_D-r|}^{r_D+r} C_A(r_A) r_A\, \mathrm{d}r_A\right] r\, \mathrm{d}r\right) \qquad (9)$$

where V_s is the micelle core volume, τ_D is the intrinsic fluorescence lifetime of the excited donor and the encounter radius, R_e, is the minimum distance between donor and acceptor at which the effect of energy transfer can still be observed in the donor fluorescence. It is usually set equal to the sum of the donor and acceptor van der Waals radii. The integration over r in eq 9 is calculated from R_e to about 3 R_0, since $w(r)$ is a very sharply peaked function of r for all accessible experimental times.[46]

The distribution functions of donor and acceptor, $C_D(r)$ and $C_A(r)$, are uniform inside the micelle core and zero outside. They can be given by a Heaviside function $H(R_{core} - r)$, which in the case of the acceptor must be multiplied by the number of acceptors per micelle n_A. For the donor we can use $C_D(r) = H(R_{core} - r)$ since the fluorescence decay profile is not determined in terms of absolute intensity.

Since anthracene is very hydrophobic and has a very limited solubility in water, we consider that all the anthracene is present in the PDcA micelle core. However, the number of anthracene molecules is not the same in all the micelles. As pointed out by Tachiya,[71] this number obeys a Poisson distribution with a mean equal to the average number of dyes per micelle. Therefore, eqs 8,9 should be calculated for all the different numbers of acceptor dyes per micelle (x) given by the Poisson distribution for a given mean number of acceptors per micelle (n_A):

$$P(x, n_A) = \frac{e^{-n_A} {n_A}^x}{x!} \tag{10}$$

Then, the resulting decay curves are each weighted with the corresponding $P(x,n_A)$ factor and summed to give the donor survival probability.

$$I_D(t) = \sum_{x=1}^{\infty} \left[P(x, n_A) \exp\left(-\frac{t}{\tau_D}\right) \int_{V_s} C_D(r_D) \varphi(t, r_D, x) {r_D}^2 \, dr_D \right] \tag{11}$$

$$\varphi(t, r_D, x) = \exp\left(-\frac{2\pi x}{r_D} \int_{R_e}^{\infty} \{1 - \exp[-w(r)t]\} \left[\int_{|r_D - r|}^{r_D + r} H(R_{core} - r_A) r_A \, dr_A \right] r \, dr \right) \tag{12}$$

In Figure 6, we show the experimental donor fluorescence decay profile measured for a micelle dispersion obtained from CP4 (0.733 g/L). The curve could only be fitted by a double exponential function, with a short component τ_{D1} = 13.4 ns and a long component τ_{D2} = 45.5 ns, with corresponding pre-exponential factors $a_1/a_2 = 0.2$. The integrated weight of the shorter component is $(a_1\tau_1)/(a_1\tau_1 + a_2\tau_2) = 4\%$. The two lifetimes probably correspond to two excited states of phenanthrene,[72] the shorter lived not usually detected when the dye have high mobility. Analysis of FRET involving a nonmonoexponential donor dye has recently been proposed, using a phenomenological approach to calculate an effective Förster radius.[73] Here, we postulate that the two phenanthrene states have the same fluorescence emission spectra, since no change is visible in the spectra when the phenanthrene shows either one or two lifetimes. In this case, the two states will have similar Förster critical radius R_0 and orientation parameter κ^2, so that, according to eq 7, the rate

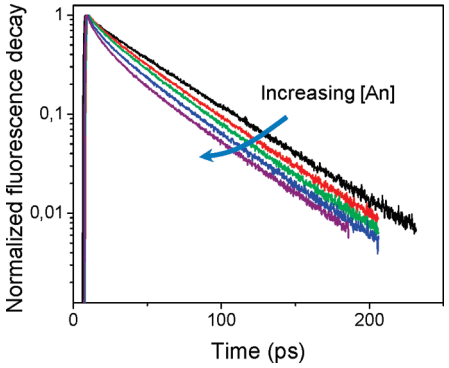

Figure 6. Experimental donor decay profiles measured for micelle dispersions of polymer CP4 (0.733 g/L) in water at 20 °C and several anthracene concentrations: (black line) 0 M; (red line) 8.5×10^{-7} M; (green line) 1.1×10^{-6} M; (blue line) 1.7×10^{-5} M; and (purple line) 8.4×10^{-5} M.

of energy transfer $w(r)$ between phenanthrene and anthracene will be much faster for the shorter lived phenanthrene state.

In order to account for the transfer from the two states of the phenanthrene we modify the donor decay eqs 11 and 12 by introducing the parameters a_1 and a_2 that weight the contribution of the rate of energy transfer (eq 7) from the two states $w_1(r)$ and $w_2(r)$, calculated for the donor decay times from each state τ_{D1} and τ_{D2}

$$I_D(t) = \sum_{x=1}^{\infty} \left\{ P(x, n_A) \int_{V_s} C_D(r_D) \left[a_1 \varphi_1(t, r_D, x) \exp\left(-\frac{t}{\tau_{D1}}\right) + a_2 \varphi_2(t, r_D, x) \exp\left(-\frac{t}{\tau_{D2}}\right) \right] {r_D}^2 \, dr_D \right\} \tag{13}$$

$$\varphi_i(t, r_D, x) = \exp\left(-\frac{2\pi x}{r_D} \int_{R_e}^{\infty} \{1 - \exp[-w_i(r)t]\} \left[\int_{|r_D - r|}^{r_D + r} H(R_{core} - r_A) r_A \, dr_A \right] r \, dr \right); \quad i = 1, 2 \tag{14}$$

The experimental donor fluorescence decay curves are analyzed by first simulating the donor survival probability curves using eqs 13 and 14. This procedure allow us to predict how the changes in the micelle core radius affect the energy transfer between the donor dyes attached to the polymer block in the micelle core and the acceptor dyes loaded into the micelle core. Some of the parameters in eqs 13,14 can be fixed to values determined independently. For the dipole orientation factor, we used the value calculated for randomly oriented transition dipole fixed during the energy transfer time scale, $\kappa^2 = 0.476$.[46] The critical Förster radius for the pair phenanthrene-anthracene has been determined as $R_0 = 2.3$ nm[47] and the donor fluorescence lifetimes for the two phenanthrene states were measured for micelles containing only donors: τ_{D1} = 13.4 ns and τ_{D2} = 45.5 ns. We also used a cutoff distance in the integration of eq 14, $R_e = 0.5$ nm,[74] because for very small donor−acceptor distances the energy transfer efficiency is so high that cannot be detected in the experimental time scale used. Finally, the number of anthracene molecules in each micelle obeys a Poisson distribution (eq 10) with mean value n_A equal to the average number of dyes *per* micelle, calculated from the mass balance of the micelle dispersions (Figure 7).

To analyze the experimental donor fluorescence decay curves we first simulated donor fluorescence decay profiles

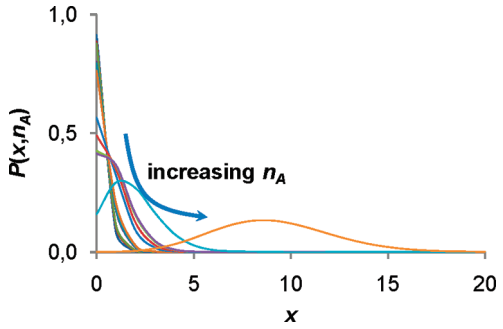

Figure 7. Effective anthracene loading in each micelle. This is given by the Poisson distribution (eq 10), with mean value n_A equal to the average number of dyes per micelle, calculated from the mass balance of the micelle dispersions.

for different values of the core radius R_{core} (from 0.5 to 12 nm) and of the mean number of acceptors per micelle n_A (related to the concentration of anthracene loaded into the micelles, Table 2), while maintaining constant $\kappa^2 = 0.476$, $R_0 = 2.3$ nm, $R_e = 0.5$ nm, and the lifetimes of the two donor states, τ_{D1} and τ_{D2}. These curves were then convoluted with the experimental instrument response functions $L(t)$ relative to each experiment,[75]

$$I_D^{conv}(t) = a \int_0^t L(s) I_D(t-s)\, \mathrm{d}s \qquad (15)$$

to obtain simulated donor fluorescence decay profiles. This library of $I_D{}^{conv}(t)$ curves was systematically compared with the corresponding experimental donor decay curves $I_D{}^{exp}(t)$ using a linear reconvolution algorithm. The fitting equation is

$$I_D^{\exp}(t) = a_1 I_{D1}^{conv}(t) + a_2 I_{D1}^{conv}(t) \qquad (16)$$

where the only fitting parameters are the decay-intensity-normalization factors a_1 and a_2 relative to the two donor states. To evaluate the quality of the fitting results, we calculated the reduced χ^2, the weighted residuals, and the autocorrelation of residuals.

In Figure 8 we show the ratio a_1/a_2 (eq 16) and the micelle core radius R_{core}, recovered for different anthracene loads in micelles of CP4. The average value recovered for the ratio $a_1/a_2 = 0.3 \pm 0.1$ is in good agreement with the corresponding ratio obtained for the fluorescence decay analysis of the micelles containing only donor ($a_1/a_2 = 0.2$) This result confirms the supposition that the two phenanthrene states have identical R_0 values, and therefore although the energy transfer kinetics is different due to the different fluorescence lifetimes of the two states, the contributions of the two states to the fluorescence decay are independent but equally affected by the acceptor distribution around each donor. This method is very useful to analyze FRET data in systems where the phenanthrene decay is not monoexponential, a common situation in phenanthrene labeled polymer systems.[76]

The micelle core radius R_{core}, (Figure 8) do not change with the average number of anthracene molecules *per* micelle within the experimental conditions used, with the mean value R_{core}(FRET) = 2.7 ± 0.1 being only slightly lower than the value obtained from the analyses of the DLS results for micelles with different corona lengths, R_{core}(DLS) = 3.0 nm. This is a clear indication that the anthracene loading does not affect the micelle core in a detectable way. Although the 10% difference between the values is probably within experimental error (it is not possible to calculate the error associated

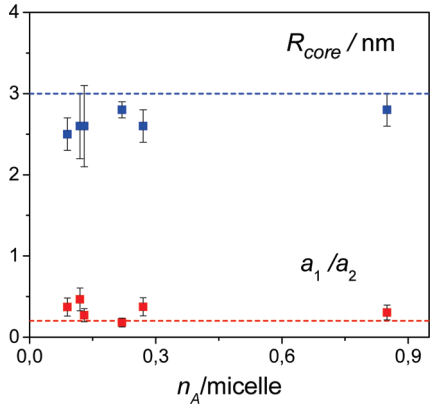

Figure 8. The micelle core radius R_{core} (red box) and the pre-exponential ratio a_1/a_2 (blue box) of eq 16, recovered from the FRET analysis of anthracene loaded CP4 micelles in water, do not change with the average number of anthracene molecules *per* micelle. The mean values of the parameters, $a_1/a_2 = 0.30.1$ and $R_{core} = 2.70.1$ are in good agreement with the value of core radius obtained by extrapolation with the star-micelle model and the pre-exponential factors of the donor fluorescence decay in the absence of acceptor (*dashed lines*).

with the core radius obtained by nonlinear extrapolation using the star micelle model), the fact that the core radius obtained by FRET is lower than the value obtained by DLS might indicate that the dyes do not occupy the area close to the core−corona interface of the micelle due to the constrains imposed by the conformations of the p(DcA) block in the micelle core.

Conclusions

Block copolymers of PDcA-PDEA, with different PDEA block lengths and a constant PDcA block labeled with a phenanthrene fluorescent dye at the α-chain-end were prepared by RAFT. These copolymers form star-like micelles in water, with a PDcA insoluble core surrounded by a PDEA corona showing thermoresponsive properties.

The micelle size was obtained from light scattering measurements for a series of micelle samples prepared from block copolymers with a constant hybrophobic PDcA core-forming block and PDEA blocks of different sizes in the corona. The aggregation number of the micelles was found not to change with the size of the solvent swollen thermoresponsive PDEA block, depending solely on the micelle core forming block. Application of a model for star-like micelles yields an estimated micelle core size, R_{core}(DLS) = 3.0 nm, and a solvent−corona interaction parameter that changes slightly with temperature due to the thermoresponsive nature of PDEA.

In the micelles, the phenanthrene at the PDcA α-chain-end becomes confined in the micelle hydrophobic core and shows two different fluorescence lifetimes. Loading anthracene into the micelle core leads to resonance energy transfer (FRET) from the core-bound excited phenanthrene to anthracene. We modified the distribution model for FRET in restricted geometries to account for the Poisson distribution of the acceptors in the micelle population and the existence of two phenanthrene states with different fluorescence lifetimes. Using this model we were able to calculated the size of the micelle core, obtaining a radius R_{core}(FRET) = 2.7 ± 0.1, very similar to the value obtained by extrapolation of the DLS data using the start micelle model for micelles with different corona lengths, R_{core}(DLS) = 3.0 nm.

We show that FRET and DLS measurements can give more information about micellar structures than usually encountered in published studies using these techniques. While both techniques yielded equivalent estimates of the micelle core radius

without deuteration of the core polymer block (as needed in neutron scattering experiments), the two types of measurements involve different sample requirements. To determine the core radius of a block copolymer star micelle in water from DLS measurements, one needs to use a series of copolymers with the same hydrophobic block length and corona forming blocks of different sizes. On the other hand, FRET measurements require only that the fluorescent donor probe and the corresponding acceptor probe be localized in the micelle core, either covalently attached to the polymer, or dissolved in the core domain. By using an appropriate FRET model one can then recover the core size with much better precision than by extrapolating the micelle size obtained by DLS using the star micelle model.

Acknowledgment. This work was partially supported by Fundação para a Ciência e a Tecnologia (FCT, Portugal) and POCI 2010 (FEDER) within project PDCT/CTM/68451/2006. The authors thank Dr. Aleksander Fedorov (CQFM-IN) for technical assistance with the picosecond lifetime measurements. Gema Marcelo and Telmo Prazeres also thank FCT for postdoc grants (SFRH/BPD/42470/2007 and SFRH/BPD/27175/2006).

References and Notes

(1) Kwon, G. S.; Kataoca, K. *Adv. Drug. Deliv. Rev.* **1995**, *16*, 295.
(2) Karymov, M.; Prochazka, K.; Mendenhal, J.; Martin, T. J.; Munk, P.; Webber, S. E. *Langmuir* **1996**, *12*, 4748.
(3) Riess, G. *Prog. Polym. Sci.* **2003**, *28*, 1107. Wiradharma, N.; Zhang, Y.; Venkataraman, S. *Nano Today* **2009**, *4*, 302. Zhou, Y. F.; Yan, D. Y. *Chem. Commun.* **2009**, *10*, 1172. Park, S.; Kim, B.; Cirpan, A.; Russell, T. P. *small* **2009**, *5*, 1343.
(4) Desponds, A.; Freitag, R. *Langmuir* **2003**, *19*, 6261.
(5) Khoukh, S.; Oda, R.; Labrot, T.; Perrin, P.; Tribet, C. *Langmuir* **2007**, *23*, 94.
(6) Prazeres, T. J. V.; Santos, A. M.; Martinho, J. M. G.; Elaïssari, A.; Pichot, C. *Langmuir* **2004**, *20*, 6834.
(7) Chung, J. E.; Yokoyama, M.; Suzuki, K.; Aoyagi, T.; Sakurai, Y.; Okano, T. *Colloids Surf, B: Biointerfaces* **1997**, *9*, 37.
(8) Qin, S.; Geng, Y.; Discher, D. E.; Yang, S. *Adv. Mater.* **2006**, *18*, 2905.
(9) Gil, E. S.; Hudson, S. A. *Prog. Polym. Sci.* **2004**, *29*, 1173.
(10) Maeda, Y.; Nakamura, T.; Ikeda, I. *Macromolecules* **2001**, *34*, 1391. Maeda, Y.; Yamamoto, H.; Ikeda, I. *Langmuir* **2001**, *17*, 6855. Ito, D.; Kubota, K. *Macromolecules* **1997**, *30*, 7828.
(11) Maeda, Y.; Nakamura, T.; Ikeda, I. *Macromolecules* **2002**, *35*, 10172.
(12) Wu, C.; Wang, X. H. *Phys. Rev. Lett.* **1998**, *80*, 4092. Wu, C.; Zhou, S. Q. *Macromolecules* **1995**, *28*, 5388. Wu, C.; Zhou, S. Q. *Macromolecules* **1995**, *28*, 8381.
(13) Schild, H. G. *Prog. Polym. Sci.* **1992**, *17* (2), 163–249.
(14) Wadajkar, A. S.; Koppolu, B.; Rahimi, M.; Nguyen, K. T. *J. Nanopart Res* **2009**, *11*, 1375. Vihola, H.; Marttila, A.-K.; Pakkanen, J. S.; Andersson, M.; Laukkanen, A.; Kaukonen, A. M.; Tenhu, H.; Hirvonen, J. *Int. J. Pharm.* **2007**, *343*, 238. Vihola, H.; Laukkanen, A.; Valtola, L.; Tenhu, H.; Hirvonen, J. *Biomaterials* **2005**, *26*, 3055.
(15) Obeid, R.; Maltseva, E.; Thunemann, A. F.; Tanaka, F.; Winnik, F. M. *Macromolecules* **2009**, *42*, 2204.
(16) Bromberg, L.; Levin, G. *Bioconjugate Chem.* **1998**, *9*, 40.
(17) Panayiotou, M.; Freitag, R. *Polymer* **2005**, *46*, 615. Panayiotou, M.; Freitag, R. *Polymer* **2005**, *46*, 6777.
(18) Liu, H. Y.; Zhu, X. X. *Polymer* **1999**, *40*, 6985.
(19) Freitag, R.; Baltes, T.; Eggert, M. J. *Polym. Sci. A: Polym. Chem.* **1994**, *32*, 3019.
(20) Idziak, I.; Avoce, D.; Lessard, D.; Gravel, D.; Zhu, X. X. *Macromolecules* **1999**, *32*, 1260.
(21) Kobayashi, M.; Ishizone, T.; Nakahama, S. *Macromolecules* **2000**, *33*, 4411.
(22) Lessard, D. G.; Ousalem, M.; Zhu, X. X.; Eisenberg, A.; Carreau, P. J. *J. Polym. Sci. B: Polym. Phys.* **2003**, *41*, 1627.
(23) Baltes, T.; Garret-Flaudy, F.; Freitag, R. *J. Polym. Sci. A: Polym. Chem.* **1999**, *37*, 2977.
(24) Siu, M. H.; Liu, H. Y.; Zhu, X. X.; Wu, C. *Macromolecules* **2003**, *36*, 2103.
(25) Pruitt, J. D.; Husseini, G.; Rapoport, N.; Pitt, M. G. *Macromolecules* **2000**, *33*, 9306.
(26) Wang, Z.; Song, Z. J.; Zhu, X. X. *J. Polym. Sci. A: Polym. Chem.* **2003**, *41*, 1681.
(27) Bromberg, L.; Levin, G. *Macromol. Rapid Commun.* **1998**, *19*, 79.
(28) Albarghouthi, M.; Buchholz, B. A.; Doherty, E. A. S.; Bogdan, F. M.; Zhou, H. H.; Barron, A. E. *Electrophoresis* **2001**, *22*, 737.
(29) Relogio, P.; Charreyre, M. T.; Farinha, J. P. S.; Martinho, J. M. G.; Pichot, C. *Polymer* **2004**, *45*, 8639.
(30) Chen, M.; Ghiggino, K. P.; Mau, A. W. H.; Rizzardo, E.; Thang, S. H.; Wilson, G. J. *Chem. Commun.* **2002**, 2276.
(31) Chen, M.; Ghiggino, K. P.; Mau, A. W. H.; Rizzardo, E.; Sasse, W. H. F.; Thang, S. H.; Wilson, G. J. *Macromolecules* **2004**, *37*, 5479.
(32) Chen, M.; Ghiggino, K. P.; Mau, A. W. H.; Sasse, W. H. F.; Thang, S. H.; Wilson, G. J. *Macromolecules* **2005**, *38*, 3475.
(33) Zhou, N.; Lu, L.; Zhu, J.; Yang, X.; Wang, X.; Zhu, X.; Zhang, Z. *Polymer* **2007**, *48*, 1255.
(34) Zhou, N. C.; Lu, L. D.; Zhu, X. L.; Yang, X. J.; Wang, X.; Zhu, J.; Zhou, D. *Polym. Bull.* **2006**, *57*, 491.
(35) Chen, M.; Ghiggino, K. P.; Launikonis, A.; Mau, A. W. H.; Rizzardo, E.; Sasse, W. H. F.; Thang, S. H.; Wilson, G. J. *J. Mater. Chem.* **2003**, *13*, 2696.
(36) Favier, A.; Charreyre, M. T. *Macromol. Rapid Commun.* **2006**, *27*, 653. Bathfield, M.; D'Agosto, F.; Spitz, R.; Charreyre, M. T.; Delair, T. *J. Am. Chem. Soc.* **2006**, *128*, 2546.
(37) Favier, A.; D'Agosto, F.; Charreyre, M. T.; Pichot, C. *Polymer* **2004**, *45*, 7821.
(38) Vagberg, L.; Cogan, K.; Gast, A. *Macromolecules* **1991**, *24*, 1670.
(39) Farinha, J. P. S.; d'Oliveira, J. M. R.; Martinho, J. M. G.; Xu, R.; Winnik, M. A. *Langmuir* **1998**, *14*, 2291.d'Oliveira, J. M. R.; Martinho, J. M. G.; Xu, R.; Winnik, M. A. *Macromolecules* **1995**, *28*, 4750 and references therein.
(40) Glatter, O.; Scherf, G.; Schillén, K.; Brown, W. *Macromolecules* **1994**, *27*, 6046.
(41) Mortensen, K.; Brown, W.; Almdal, K.; Alami, E.; Jada, A. *Langmuir* **1997**, *13*, 3635.
(42) Zhang, L.; Eisenberg, A. *Science* **1995**, *268*, 1728. Zhang, L.; Eisenberg, A. *J. Am. Chem. Soc.* **1996**, *118*, 3168. Yu, Y.; Zhang, L.; Eisenberg, A. *Macromolecules* **1998**, *31*, 1144.
(43) Berberan-Santos, M. N.; Prieto, M. J. E. *J. Chem. Soc., Faraday Trans. 2* **1987**, *83*, 1391. Duhamel, J.; Yekta, A.; Ni, S.; Khaykin, Y.; Winnik, M. A. *Macromolecules* **1993**, *26*, 6255. Martin, T. J.; Webber, S. E. *Macromolecules* **1995**, *28*, 8845. Schillén, K.; Yekta, A.; Ni, S.; Winnik, M. A. *Macromolecules* **1998**, *31*, 210.
(44) Klafter, J.; Blumen, A. *J. Chem. Phys.* **1984**, *80*, 875.
(45) Farinha, J. P. S.; Spiro, J.; Winnik, M. A. *J. Phys. Chem. B* **2001**, *105*, 4879.
(46) Farinha, J. P. S.; Martinho, J. M. G. *J. Phys. Chem. C* **2008**, *112*, 10591.
(47) Farinha, J. P. S.; Martinho, J. M. G.; Kawagushi, S.; Yekta, A.; Winnik, M. A. *J. Phys. Chem.* **1996**, *100*, 12552.
(48) Yekta, A.; Winnik, M. A.; Farinha, J. P. S.; Martinho, J. M. G. *J. Phys. Chem. A* **1997**, *101*, 1787.
(49) Farinha, J. P. S.; Martinho, J. M. G. *J. Lumin.* **1997**, *72*, 914.
(50) Farinha, J. P. S.; Relógio, P.; Charreyre, M.-T.; Prazeres, T. J. V.; Martinho, J. M. G. *Macromolecules* **2007**, *40*, 4680.
(51) Afonso, C. A. M.; Farinha, J. P. S. *J. Chem. Res., Synop.* **2002**, 584.
(52) Prazeres, T. J. V.; Beija, M.; Charreyre, M.-T.; Farinha, J. P. S.; Martinho, J. M. G. *Polymer* **2009**, in press.
(53) Gonçalves da Silva, A. M.P.S.; Lopes, S. I.C.; Brogueira, P.; Prazeres, T. J. V.; Beija, M.; Martinho, J. M. G. *J. Colloid Interface Sci.* **2008**, *327*, 129.
(54) Favier, A.; Charreyre, M. T.; Pichot, C. *Polymer* **2004**, *45*, 8661.
(55) Favier, A.; Ladaviere, C.; Charreyre, M. T.; Pichot, C. *Macromolecules* **2004**, *37*, 2026.
(56) Itakura, M.; Inomata, K.; Nose, T. *Polymer* **2000**, *41*, 8681.
(57) Chu, B. *Laser Light Scattering: Basic Principles and Practice*, 2nd ed.; Academic Press: San Diego, CA, 1991.
(58) Stepanek, P. In *Dynamic Light Scattering: The Method and Some Applications*; Brown, W., Ed.; Oxford University Press: Oxford, U.K., 1993.
(59) Cummins, H. Z.; Pusey, P. N. In *Photon Correlation Spectroscopy and Velocimetry*; Cummins, H. Z., Pike, E. R., Eds.; Plenum Press: New York, 1977.
(60) Prazeres, T. J. V.; Farinha, J. P. S.; Martinho, J. M. G. *J. Phys. Chem. C* **2008**, *112*, 1633.
(61) Rechthaler, K.; Kohler, G. *Chem. Phys.* **1994**, *189*, 99.
(62) Jones, G.II; Jackson, W. R.; Kanoktanaporn, S.; Halpern, A. M. *Opt. Commun.* **1980**, *33*, 315.

(63) Horng, M. L.; Gardecki, J. A.; Papazyan, A.; Maroncelli, M. *J. Phys. Chem.* **1995**, *99*, 17311.
(64) Becker, R. S.; Chakravorti, S.; Gartner, C. A.; Miguel, M. D. *J. Chem. Soc. Faraday Trans.* **1993**, *89*, 1007.
(65) Zimm, B J. *Chem. Phys.* **1948**, *16*, 1093.
(66) Yamakawa, H. *Modern Theory of Polymer Solutions*; Harper & Row: New York, 1971.
(67) King, T. A.; Treadaway, M. F. *J. Chem. Soc., Faraday Trans. 2* **1977**, *73*, 1616–1626.
(68) Zhang, L.; Barlow, R. J.; Eisenberg, A. *Macromolecules* **1995**, *28*, 6055.
(69) Förster, Th *Ann. Phys.* (*Leipzig*) **1948**, *2*, 55. Förster, Th *Z. Naturforsch.* **1949**, *4a*, 321.
(70) Baumann, J.; Fayer, M. D. *J. Chem. Phys.* **1986**, *85*, 4087.
(71) Tachiya, M. *Chem. Phys. Lett.* **1975**, *33*, 289.
(72) Azumi, T.; McGlynn, S. P. *J. Chem. Phys.* **1962**, *37*, 2413.
(73) Felorzabihi, N.; Froimowicz, P.; Haley, J. C.; Bardajee, G. R.; Li, B. X.; Bovero, E.; van Veggel, F. C. J. A.; Winnik, M. A. *J. Phys. Chem. B* **2009**, *113*, 2262.
(74) Farinha, J. P. S.; Schillen, K.; Winnik, M. A. *J. Phys. Chem. B* **1999**, *103*, 2487.
(75) Farinha, J. P. S.; Martinho, J. M. G.; Pogliani, L. *J. Math. Chem.* **1997**, *21*, 131.
(76) Liu, Ronghua; Farinha, J. P. S.; Winnik, M. A. *Macromolecules* **1999**, *32*, 3957.